JAERI-Tech
94-022

CRITICAL ELEMENT STUDY ON AUTONOMOUS POSITION CONTROL OF ARTICULATED-ARM TYPE MANIPULATOR

October 1994

Kiyoshi OKA, Satoshi KAKUDATE, Masataka NAKAHIRA
Eisuke TADA, Kenjiro OBARA, Kou TAGUCHI, Naokazu KANAMORI
Mitsunori KONDOH, Kiyoshi SHIBANUMA and Masahiro SEKI

日本原子力研究所
Japan Atomic Energy Research Institute

本レポートは，日本原子力研究所が不定期に公刊している研究報告書です。
入手の問合わせは，日本原子力研究所技術情報部情報資料課（〒319－11 茨城県那珂郡東海村）あて，お申し越しください。なお，このほかに財団法人原子力弘済会資料センター（〒319－11 茨城県那珂郡東海村日本原子力研究所内）で複写による実費頒布をおこなっております。

This report is issued irregularly.
Inquiries about availability of the reports should be addressed to Information Division, Department of Technical Information, Japan Atomic Energy Research Institute, Tokai-mura, Naka-gun, Ibaraki-ken 319-11, Japan.

編集兼発行　日本原子力研究所
印　　刷　日立高速印刷株式会社

JAERI-Tech 94-022

Critical Element Study on Autonomous Position Control of Articulated-arm Type Manipulator

Kiyoshi OKA, Satoshi KAKUDATE, Masataka NAKAHIRA
Eisuke TADA, Kenjiro OBARA, Kou TAGUCHI
Naokazu KANAMORI, Mitsunori KONDOH+
Kiyoshi SHIBANUMA+ and Masahiro SEKI

Department of Fusion Engineering Research
Naka Fusion Research Establishment
Japan Atomic Energy Research Institute
Naka-machi, Naka-gun, Ibaraki-ken

(Received September 6, 1994)

An articulated-arm type manipulator can be operated effectively in a restricted space due to its flexibility and it can be attractive for a wide range of in-vessel maintenance such as viewing, inspection and limiter handling in fusion experimental reactors. In case of the in-vessel maintenance using a flexible manipulator, it is quite essential to develop an autonomous control method for compensating a deflection of manipulator so as to minimize the maintenance time with high precision.

For this purpose, a new position control method using a combination of neural network predictor with a rigid inverse kinematics is being developed. The key features of this method are to simplify a kinematics modeling of flexible manipulator, to enable quick position compensation in stead of ordinary large matrix compensation, and to be applicable to a wide variety of manipulator characteristics. A sub-scaled model of flexible manipulator with 4 joints has been fabricated for a benchmark experiments of the autonomous position control. Comparing analytical simulation with experiments using the flexible manipulator, it has been demonstrated that the new position control method gives significant

+ Department of ITER Project

improvement in control performance with high precision in order of a figure. In addition, further optimization can be possible by adding other non-linear predictors such as radial basis function and fuzzy modeling.

This paper describes the details of a sub-scaled flexible manipulator and a neural network position control system as well as results of analytical simulation and benchmark experiments.

Keywords : Fusion Experimental Reactors, In-vessel Maintenance, Articulated-arm, Autonomous Position Control, Neural Network

多関節型マニピュレータのための自律位置制御に関する要素研究

日本原子力研究所那珂研究所核融合工学部

岡　　潔・角舘　聡・中平　昌隆・多田　栄介

小原建治郎・田口　浩・金森　直和・近藤　光昇[+]

柴沼　清[+]・関　昌弘

（1994年9月6日受理）

核融合実験炉において，炉内での主な作業である炉内観察，検査及び第1壁の交換等に，多関節型マニピュレータは，幅広く利用される事が見込まれている。このマニピュレータを炉内全域にアクセスさせるためには，長い腕と多くの関節が必要となる。通常，マニピュレータを剛体とみなすことによって位置制御を行うが，この場合，自重等のたわみによって，先端位置誤差が無視できない一種の柔軟体モデルとなる。従って，柔軟なマニピュレータの手先位置を高精度に補償する位置制御が必要である。

本報告では，従来までの柔軟マニピュレータの位置制御に必要であった複雑な数学モデルを使用せず，通常の剛体モデルを基本とし，マニピュレータのたわみと関節のガタによる先端位置の誤差情報をニューラルネットワークによってあらかじめ学習しておき，補正を行うシステムを提案する。さらに，本システムの制御法の有効性は，炉内保守用マニピュレータの縮小モデルに適用することで実証され，柔軟マニピュレータを制御する一手法として，有効なデータベースを構築した。

那珂研究所：〒311－01　茨城県那珂郡那珂町向山801－1

＋　ITER開発室

目　　次

Contents

1. INTRODUCTION

The Japan Atomic Energy Research Institute (JAERI) has been conducting technology development aiming at realization of fusion experimental reactor[1,2]. Since the core of fusion reactor will be highly activated due to D-T operation, assembly and maintenance of all reactor components will have to be totally conducted by remote handling technology. In particular, the plasma facing components such as divertor, first wall and limiters are categorized into scheduled maintenance components due to their severe operating conditions and thus reliable and quick remote maintenance operation are highly required.

An articulated-arm type manipulator can be operated effectively in a restricted space due to its flexibility and it can be attractive for a wide range of in-vessel maintenance operations such as viewing, inspection and handling of limiters. In this case, however, a manipulator with a arm length of at least 6 m and a degree of freedom of 8 axes is required so as to access all of in-vessel region. Hence, an advanced control method is inevitably required to compensate a position error caused by deflection and torsion of manipulator itself since manipulator becomes rather flexible and less stiffness.

For this purpose, a new position control method using a combination of neural network[3] predictor with a rigid inverse kinematics is proposed for the in-vessel maintenance using such flexible manipulator. In this method, a neural network can predict a modeling error between a target value and a kinematics model according to a learned relation from representative points in the manipulator working space. Based on this prediction, the target position values are modified so as to reduce the total position control error using inverse kinematics. The key features of this method are summarized as follows.

(1) A simplified modeling of manipulator kinematics without a detailed model representing manipulator characteristics

(2) Quick and precise position compensation compared with ordinary method based on large matrix compensation

(3) Easy modification for variety of manipulator configuration

In order to verify the feasibility of this autonomous position control method, a sub-scaled model of flexible manipulator for simulating in-vessel maintenance has been fabricated and benchmark experiments have been conducted together with analytical simulation. As a result, it has been demonstrated that the new position control method based on neural network indicates significant improvement in control performance. In addition, further optimization can be possible by adding other non-linear predictors such as radial basis function and fuzzy modeling.

This paper describes the details of a sub-scaled flexible manipulator and a neural network position control system as well as results of analytical simulation and benchmark experiments.

2. A SUB-SCALED FLEXIBLE MANIPULATOR

Figure 1 shows typical schematic view of an in-vessel manipulator for handling limiter. According to the overall machine layout of ITER (International Thermonuclear Experimental Reactor), a minimum arm length and a degree of freedom of the manipulator are to be 6 m and 8 axes, respectively. In order to simulate those conditions and investigate the controllability based on neural network, a sub-scaled model of flexible manipulator has been fabricated. The key features of this sub-scaled manipulator are as follows.

(1) The size of manipulator is roughly 1/5 of the actual manipulator and the maximum deflection at the tip is defined to be 20 mm at a payload of 5 kg.

(2) The degree of freedom of manipulator is 4 axes: 2 axes can be replaced so as to investigate the controllability under different joint characteristics.

Figure 2 shows an overall assembly of the sub-scaled manipulator which can be operated on the surface of a vertical plate simulating first wall arrangement. The major parameters of the manipulator are summarized in **Table 1** and the design outline is described in the following paragraphs.

2-1. Measurement and control system of the manipulator

The sub-scaled manipulator is composed of 4 joints and an end-effector: the total length of manipulator arm is around 1.6 m, as shown in **Fig. 3**. For measuring the tip position of the manipulator, a CCD camera is attached at the end-effector and can view at least two of representative holes set on the vertical plate so as to find out the absolute position of the tip: a number of holes with diameter of 5 mm and 50-mm pitch are allocated on the vertical plate surface on which the manipulator is working. An image processor analyzes the absolute center position of the two representative holes detected on a CRT screen. A personal computer is used as data processing system to compute position and posture of the tip from the measured representative holes and to provide necessary commands to a robot controller for position control of the manipulator based on the measured position information. A robot controller is designed both to transmit the manipulator position information based on each joint angle to the personal computer and to operate the manipulator according to the commands provided by the personal computer as well as ordinary control function.

The manipulator is controlled by the robot controller in assistance with commands from the personal computer. The basic procedures of the position compensating control are as follows.

(1) To calculate actual position and inclination of the tip from the position data of the representative holes: the position date is characterized in the image processor and transmitted through GP-IB interface to the personal computer.

Table 1 Specification of the manipulator system

Item	Specification
Degree of freedom	θ_1 : first arm revolution θ_2 : first arm translation θ_3 : second arm revolution θ_4 : third arm revolution
Range of movement	θ_1 : over ±180 degree θ_2 : stroke of 650 mm θ_3 : +60~-180 degree θ_4 : ±120 degree
Velocity	θ_1 : 10 °/sec θ_2 : 50 mm/sec θ_3 : 10 °/sec θ_4 : 20 °/sec
Arm length	L_1 : 800 mm L_2 : 400 mm L_3 : 400 mm offset ℓ_1 : 100 mm offset ℓ_2 : 85 mm
Payload	5 kgf
Weight	30 kgf
Constitution of drive	θ_1 : DC motor + planetary gear + harmonic drive gear θ_2 : DC motor + harmonic drive gear + rack & pinion θ3 : DC motor + timing belt + harmonic drive gear θ_4 : DC motor + timing belt + harmonic drive gear
Design value of tip deflection	max : 20 mm (most extension to horizontal direction) a factor of elastic deformation is harmonic drive and arm

(2) To evaluate a relative deflection between the tip position estimated by the rigid model using joint angle data measured in the robot controller and the actual tip position specified by the viewing system.

(3) To learn the position compensation relation based on the evaluated deflection according to neural network algorithm.

(4) To predict a deflection of the tip from the learned position compensation relation, to generate the joint angle date for compensating the deflection and to transmit the joint angle data to the robot controller as a control command.

2-2. Kinematics of the manipulator in rigid model

In principle, a tip position can be analytically obtained from angle position of each joint by solving kinematics in a numerical model of a manipulator and hence a joint angle can be obtained by solving the inverse kinematics when a tip position is given.

The sub-scaled manipulator is composed of 4 joints and 3 arms as shown in Fig. 3. When the sub-scaled manipulator is assumed to be a rigid model, numerical model of the sub-scaled manipulator is specified and kinematics and inverse kinematics are defined as follows.

(1)Coordinates of each joint

$\hat{X}_0$, $\hat{Y}_0$, $\hat{Z}_0$: Base coordinates

$\hat{X}_n$, $\hat{Y}_n$, $\hat{Z}_n$: θ_n coordinates

where, $\hat{X}_n$, $\hat{Y}_n$, $\hat{Z}_n$ correspond to the manipulator axis, perpendicular to the manipulator axis in the same working plane and perpendicular to the working plane of the manipulator. θ_n indicates rotation around joints.

(2) Link parameter of the manipulator

According to the structural design of the manipulator, the characteristics matrix of the manipulator is given as shown in **Table 2**.

Table 2 Link parameter of the manipulator

i	a_{i-1}	α_{i-1}	d_i	θ_i
1	0	0°	0	θ_1+90°
2	m_1	90°	ℓ_2 (θ_2)	180°
3	m_2	90°	0	θ_3+90°
4	ℓ_3	0°	0	θ_4
5	ℓ_4	0°	0	0°

where,

a_{i-1} : a distance between $\hat{Z}_{i-1}$ and $\hat{Z}_i$ along $\hat{X}_{i-1}$
α_{i-1} : an angle between $\hat{Z}_{i-1}$ and $\hat{Z}_i$ around $\hat{X}_{i-1}$
d_i : a distance between $\hat{X}_{i-1}$ and $\hat{X}_i$ along $\hat{Z}_i$
θ_i : an angle between $\hat{X}_{i-1}$ and $\hat{X}_i$ around $\hat{Z}_i$

(3) Kinematics of the manipulator

A general kinematics is given by ${}^{i-1}_{i}T$ and thus kinematics of the manipulator is represented as follows.

$$ {}^{i-1}_{i}T = \begin{bmatrix} \cos\theta_i & -\sin\theta_i & 0 & \alpha_{i-1} \\ \sin\theta_i \cdot \cos\alpha_{i-1} & \cos\theta_i \cdot \cos\alpha_{i-1} & -\sin\alpha_{i-1} & -\sin\alpha_{i-1} \cdot d_i \\ \sin\theta_i \cdot \sin\alpha_{i-1} & \cos\theta_i \cdot \sin\alpha_{i-1} & \cos\alpha_{i-1} & \cos\alpha_{i-1} \cdot d_i \\ 0 & 0 & 0 & 1 \end{bmatrix} $$

By substituting the link parameter of the manipulator for the above equation, following equation is given as a numerical model of the manipulator to analyze the tip position from the angle data of each joint.

$$ {}^{0}_{5}T = \begin{bmatrix} {}^{0}_{5}r_{11} & {}^{0}_{5}r_{12} & {}^{0}_{5}r_{13} & {}^{0}_{5}r_{14} \\ {}^{0}_{5}r_{21} & {}^{0}_{5}r_{22} & {}^{0}_{5}r_{23} & {}^{0}_{5}r_{24} \\ {}^{0}_{5}r_{31} & {}^{0}_{5}r_{32} & {}^{0}_{5}r_{33} & {}^{0}_{5}r_{34} \\ {}^{0}_{5}r_{41} & {}^{0}_{5}r_{42} & {}^{0}_{5}r_{43} & {}^{0}_{5}r_{44} \end{bmatrix} $$

where,

$$ {}^{0}_{5}r_{11} = {}^{0}_{5}r_{22} = \cos(\theta_1 + \theta_3 + \theta_4) $$
$$ {}^{0}_{5}r_{12} = -\sin(\theta_1 + \theta_3 + \theta_4) $$
$$ {}^{0}_{5}r_{21} = \sin(\theta_1 + \theta_3 + \theta_4) $$
$$ {}^{0}_{5}r_{14} = \ell_4 \cdot \cos(\theta_1 + \theta_3 + \theta_4) + \ell_3 \cdot \cos(\theta_1 + \theta_3) - (m_1 - m_2) \cdot \sin\theta_1 + \ell_2 \cdot \cos\theta_1 $$
$$ {}^{0}_{5}r_{24} = \ell_4 \cdot \sin(\theta_1 + \theta_3 + \theta_4) + \ell_3 \cdot \sin(\theta_1 + \theta_3) + (m_1 - m_2) \cdot \cos\theta_1 + \ell_2 \cdot \sin\theta_1 $$
$$ {}^{0}_{5}r_{13} = {}^{0}_{5}r_{23} = {}^{0}_{5}r_{31} = {}^{0}_{5}r_{32} = {}^{0}_{5}r_{34} = {}^{0}_{5}r_{41} = {}^{0}_{5}r_{42} = {}^{0}_{5}r_{43} = 0 $$
$$ {}^{0}_{5}r_{33} = {}^{0}_{5}r_{44} = 1 $$

(4) Inverse kinematics of the manipulator

When the tip position/posture of the manipulator is given to be (x, y, ϕ), an inverse kinematics of the manipulator is also obtained from the above correlation, as follows.

$$x = \ell_4 \cdot \cos(\theta_1 + \theta_3 + \theta_4) + \ell_3 \cdot \cos(\theta_1 + \theta_3) + \ell_2 \cdot \cos\theta_1 - (m_1 - m_2) \cdot \sin\theta_1$$

$$y = \ell_4 \cdot \sin(\theta_1 + \theta_3 + \theta_4) + \ell_3 \cdot \sin(\theta_1 + \theta_3) + \ell_2 \cdot \sin\theta_1 + (m_1 - m_2) \cdot \cos\theta_1$$

$$\cos\phi = \cos(\theta_1 + \theta_3 + \theta_4)\ ,\ \sin\phi = \sin(\theta_1 + \theta_3 + \theta_4)$$

2-3. Mechanical characteristics of the manipulator

As mentioned previously, the sub-scaled manipulator is composed of 4 joints, 3 arms and an end-effector: the weight distribution of each part of the manipulator is listed in **Table 3.**

Table 3 Weight of each part of manipulator

First axis	11 kg	Second arm	4.81 kg
Second axis	1.4 kg	Third arm	0.19 kg
Third axis	4.25 kg	Forth arm	0.15 kg
Forth axis	2.66 kg	End effector	4.81 kg
		Total weight	29.27 kg

In order to investigate the controllability for position compensation, mechanical characteristics such as deflection, the angle of deflection, the play of joints and natural frequency have been measured prior to the analytical simulation and benchmark experiments.

(1) Deflection and backlash measurement

For the measurement of deflection, the angle of deflection and the play of joints, static loads up to ± 5 kg are applied to each part of the manipulator: the loading points (P1 ~ P13) are indicated in Fig. 3. The measured characteristics are summarized in **Table 4 and 5**. From those results, it has been confirmed that the maximum deflection of the manipulator tip is approximately 20 mm under 5-kg loading as expected in the structural design. The spring constants of the major parts such as harmonic drive and linear motion guide are different in positive and negative loading. In particular, the spring constant of harmonic drive in positive loading is much smaller than that in negative loading: this is due to a balance of dead weight canceling/accelerating by the applied loads and stiffness. The backlashes of joints are ranging from 10^{-4} to 10^{-3} rad.

(2) Natural frequency

The natural frequency of the manipulator is measured by hitting the position of end-effector as a function of payload (0.2 ~ 5 kg) and No.2 arm length (160 ~ 800 mm): this corresponds to a total arm length from 960 to 1600 mm. In this experiment, acceleration

sensors are set on the tip and the manipulator arm is positioned in the horizontal posture. The experimental results are shown in **Table 6**. The natural frequency of the manipulator is ranging from 9.93~12.41 Hz in case of a payload of 0.2 kg and 3.60~3.86 Hz at 5-kg payload.

Table 4 Maximum deflection and a play of joint

Measuring point	Maximum deflection		Looseness (mm)
	Positive load (mm/kg)	Negative load (mm/kg)	
P_1	0.15/4.5	-0.072/-4.9	0.06
P_2	0.11/4.5	-0.067/-4.9	0.03
P_3	0.12/4.5	-0.072/-4.9	0.03
P_4	1.46/4.4	-1.05/-5.1	0.28
P_5	1.63/4.4	-1.21/-5.1	0.28
P_6	1.60/4.6	-1.25/-5.3	0.35
P_7	1.88/4.6	-1.47/-5.3	0.35
P_8	4.44/4.6	-4.25/-5.3	0.58
P_9	3.73/4.3	-3.33/-4.7	0.53
P_{10}	4.96/4.3	-4.56/-4.7	0.64
P_{11}	5.80/4.3	-5.47/-4.7	0.53
P_{12}	17.5/5.1	-14.9/-4.8	2.22
P_{13}	17.5/4.8	-16.9/-4.6	2.08

Table 5 Backlash and spring constants

	Spring constant (positive area)	Spring constant (negative area)	Backlash
H.D.* of 1st axis	1.62×10^{-4} rad/kg-m	9.73×10^{-4} rad/kg-m	5.6×10^{-4} rad.
L.M.** of 2nd axis	3.26×10^{-4} rad/kg-m	2.57×10^{-4} rad/kg-m	3.8×10^{-4} rad.
Deflection of 2nd arm	0.176 mm/kg-m	0.132 mm/kg-m	
Deflected angle of 2nd arm	1.57×10^{-4} rad/kg-m	1.47×10^{-4} rad/kg-m	
H.D. of 3rd axis	7.48×10^{-4} rad/kg-m	5.43×10^{-4} rad/kg-m	5.7×10^{-4} rad.
Deflection of 3rd arm	0.73 mm/kg-m	0.68 mm/kg-m	
Deflected angle of 3rd arm	2.83×10^{-3} rad/kg-m	3.04×10^{-3} rad/kg-m	
H.D. of 4th axis	4.70×10^{-3} rad/kg-m	4.30×10^{-3} rad/kg-m	1.4×10^{-3} rad.
Deflection of 4th arm	6.70 mm/kg-m	6.58 mm/kg-m	
Deflected angle of 4th arm	1.54×10^{-2} rad/kg-m	1.74×10^{-2} rad/kg-m	

* Harmonic Drive
** Liner Motion Guide

Table 6 Natural frequency of manipulator

No.	Payload (kg)	Posture of manipulator				Natural frequency (Hz)
		θ_1 (deg.)	θ_2 (mm)	θ_3 (deg.)	θ_4 (deg.)	
1	0.2	0.0	160.0	0.0	0.0	12.41
2	0.2	0.0	400.0	0.0	0.0	11.85
3	0.2	0.0	800.0	0.0	0.0	9.93
4	5.0	0.0	160.0	0.0	0.0	3.86
5	5.0	0.0	400.0	0.0	0.0	3.77
6	5.0	0.0	800.0	0.0	0.0	3.60

3. CONTROL SYSTEM FOR POSITION COMPENSATION

3-1. Outline of position compensation

In general, an actual manipulator behaves in a different manner from expectation of the rigid model due to fabrication errors such as the play of joints, misalignment, deflection and torsion of manipulator. Accordingly, it is essential to develop a control method for

Table 5 Backlash and spring constants

	Spring constant (positive area)	Spring constant (negative area)	Backlash
H.D.* of 1st axis	1.62×10^{-4} rad/kg-m	9.73×10^{-4} rad/kg-m	5.6×10^{-4} rad.
L.M.** of 2nd axis	3.26×10^{-4} rad/kg-m	2.57×10^{-4} rad/kg-m	3.8×10^{-4} rad.
Deflection of 2nd arm	0.176 mm/kg-m	0.132 mm/kg-m	
Deflected angle of 2nd arm	1.57×10^{-4} rad/kg-m	1.47×10^{-4} rad/kg-m	
H.D. of 3rd axis	7.48×10^{-4} rad/kg-m	5.43×10^{-4} rad/kg-m	5.7×10^{-4} rad.
Deflection of 3rd arm	0.73 mm/kg-m	0.68 mm/kg-m	
Deflected angle of 3rd arm	2.83×10^{-3} rad/kg-m	3.04×10^{-3} rad/kg-m	
H.D. of 4th axis	4.70×10^{-3} rad/kg-m	4.30×10^{-3} rad/kg-m	1.4×10^{-3} rad.
Deflection of 4th arm	6.70 mm/kg-m	6.58 mm/kg-m	
Deflected angle of 4th arm	1.54×10^{-2} rad/kg-m	1.74×10^{-2} rad/kg-m	

* Harmonic Drive
** Liner Motion Guide

Table 6 Natural frequency of manipulator

No.	Payload (kg)	Posture of manipulator				Natural frequency (Hz)
		θ_1 (deg.)	θ_2 (mm)	θ_3 (deg.)	θ_4 (deg.)	
1	0.2	0.0	160.0	0.0	0.0	12.41
2	0.2	0.0	400.0	0.0	0.0	11.85
3	0.2	0.0	800.0	0.0	0.0	9.93
4	5.0	0.0	160.0	0.0	0.0	3.86
5	5.0	0.0	400.0	0.0	0.0	3.77
6	5.0	0.0	800.0	0.0	0.0	3.60

3. CONTROL SYSTEM FOR POSITION COMPENSATION

3-1. Outline of position compensation

In general, an actual manipulator behaves in a different manner from expectation of the rigid model due to fabrication errors such as the play of joints, misalignment, deflection and torsion of manipulator. Accordingly, it is essential to develop a control method for

compensating such deflection and torsion caused by the dead weight of manipulator, resulting in accurate and quick in-vessel maintenance using a flexible manipulator.

In order to compensate a position error theoretically, it is required to establish a detailed numerical kinematics model representing the flexible manipulator characteristics and to analyze an inverse kinematics of the detailed model. However, it is hard to establish such numerical model with non-rigid functions in an actual flexible manipulator. Even if such a numerical model is defined, it is impractical to solve analytically the complex inverse kinematics using large and high speed computer system with wasting an enormous time.

An approximate prediction has been proposed as a practical method in stead of the above numerical method so as to compensate the deflection with a reasonable precision. In this method, the basic procedures are as follows.

(1) A deflection of manipulator is modeled as non-linear characteristics.

(2) A target position of manipulator is renewed according to the predicted deflection from the non-linear model.

(3) Joint angles of manipulator are obtained from an inverse kinematics of the rigid model so as to move the manipulator to the renewed position.

There are several possible modeling methods to predict a non-linear deflection. A neural network is a candidate method with attractive features such as simplicity for high dimensional system and adaptability to interface variation, although it has disadvantages in learning duty and difficulty of analyses on internal process. The following paragraphs describe a position compensating control system based on a neural network for predicting a deflection.

3-2. Control algorithm for position compensation

Figure 4 shows a typical block diagram of position compensating control based on a neural network. A nominal value of joint angle (θ_0) is calculated from a inverse kinematics of the rigid model in order to satisfy a target value ($\mathbf{x}_d$) of the tip position/posture. A deflection (Δ_N) of manipulator is estimated from a neural network predictor when a manipulator is moved along the nominal angle (θ_0) calculated. Based on the predicted deflection value(Δ_N) and the following equation, a final position/posture (x^*) of the tip is renewed so as to minimize an error between a target value and actual value. A final joint angle (θ^*) of manipulator can be obtained again from an inverse kinematics of the rigid model according to the final position/posture (x^*).

$$x^* = x_d - \Delta_N(\theta_0)$$

Since this compensating procedure is iterative, the accuracy of position/posture control is improved with increase in iteration within the following constraints.

(1) An angle of displacement vectors between actual manipulator and rigid model is less than 60 degree if the both displacement vectors are the same order of magnitude.

(2) A displacement vector of actual manipulator is less than 2 times of rigid model displacement if the both displacement vector is oriented in the same direction.

4. ANALYTICAL SIMULATION

4-1. Simulation scheme

In order to verify the basic feasibility of a neural network control for position compensation, an analytical simulation based on the design features of the sub-scaled manipulator has been conducted. Since the manipulator is composed of 4 joints and 3 arms supported by the first joint, the deflection of the manipulator arm can be estimated from a numerical model with a beam and canti-lever type support.

In this simulation, a working space and a target position of the manipulator tip is assumed as shown in **Fig. 5** and the No.2 arm length is fixed to be 600 mm. In such a situation, a number of joint angle data is selected at random and an error between the predicted tip position and the estimated tip position from the rigid model is calculated so that compensating relation between joint angle and error of the tip position is learned based on a neural network . The detailed simulation processes are described below.

(1) To specify a target position/posture data : $\mathbf{x}_d = (x_d, y_d, \phi_d)$.
(2) To calculate the corresponding joint angle from inverse kinematics of rigid model : θ_{d0}
(3) To predict a deflection($\Delta_N(\theta_{d0})$) and a tip position by neural network ($\mathbf{x}_0(\theta_{d0})$)
(4) To renew the target position/posture : $\tilde{\mathbf{x}}_d = \mathbf{x}_d - \Delta_N(\theta_{d0})$
(5) To calculate a joint angle (θ_{d1}) for the renewed target from inverse kinematics of rigid model.
(6) To calculate a tip position $\mathbf{x}_1(\theta_{d1})$ when a joint angle is (θ_{d1}).

where,

$\Delta_N(\theta_{d0})$: a predictive deflection at nominal joint angle θ_{d0}.

$\mathbf{x}_0(\theta_{d0})$: a tip position of actual model at nominal joint angle θ_{d0}.

$\tilde{\mathbf{x}}_d$: a renewed target position/posture for compensating control.

$\mathbf{x}_1(\theta_{d1})$: a tip position of actual model at a renewed joint angle (θ_{d1}).

4-2. Simulation results

(1) Sensitivity on prediction error

In a neural network, the prediction precision will depend on the number of data set and unit of the network layer. In order to clarify such dependency and to optimize the neural network conditions, the fitting precision is investigated as a function of the number of data set and unit of the neural network layer.

(2) A displacement vector of actual manipulator is less than 2 times of rigid model displacement if the both displacement vector is oriented in the same direction.

4. ANALYTICAL SIMULATION

4-1. Simulation scheme

In order to verify the basic feasibility of a neural network control for position compensation, an analytical simulation based on the design features of the sub-scaled manipulator has been conducted. Since the manipulator is composed of 4 joints and 3 arms supported by the first joint, the deflection of the manipulator arm can be estimated from a numerical model with a beam and canti-lever type support.

In this simulation, a working space and a target position of the manipulator tip is assumed as shown in **Fig. 5** and the No.2 arm length is fixed to be 600 mm. In such a situation, a number of joint angle data is selected at random and an error between the predicted tip position and the estimated tip position from the rigid model is calculated so that compensating relation between joint angle and error of the tip position is learned based on a neural network . The detailed simulation processes are described below.

(1) To specify a target position/posture data : $\mathbf{x}_d = (x_d, y_d, \phi_d)$.
(2) To calculate the corresponding joint angle from inverse kinematics of rigid model : θ_{d0}
(3) To predict a deflection($\Delta_N(\theta_{d0})$) and a tip position by neural network ($\mathbf{x}_0(\theta_{d0})$)
(4) To renew the target position/posture : $\tilde{\mathbf{x}}_d = \mathbf{x}_d - \Delta_N(\theta_{d0})$
(5) To calculate a joint angle (θ_{d1}) for the renewed target from inverse kinematics of rigid model.
(6) To calculate a tip position $\mathbf{x}_1(\theta_{d1})$ when a joint angle is (θ_{d1}).

where,

$\Delta_N(\theta_{d0})$: a predictive deflection at nominal joint angle θ_{d0}.

$\mathbf{x}_0(\theta_{d0})$: a tip position of actual model at nominal joint angle θ_{d0}.

$\tilde{\mathbf{x}}_d$: a renewed target position/posture for compensating control.

$\mathbf{x}_1(\theta_{d1})$: a tip position of actual model at a renewed joint angle (θ_{d1}).

4-2. Simulation results

(1) Sensitivity on prediction error

In a neural network, the prediction precision will depend on the number of data set and unit of the network layer. In order to clarify such dependency and to optimize the neural network conditions, the fitting precision is investigated as a function of the number of data set and unit of the neural network layer.

Table 7 shows the dependency of fitting precision on the number of unit. In this analysis, the number of unit is varied from 5 to 15 and total number of data set is fixed to be 50. From this analysis, a minimum number of the unit is selected to be 10. Based on this, a prediction ability is investigated with a variety of the number of data set ranging from 30 to 50. The results are shown in **Table 8** and it is concluded that at least 40 pair of data set is required to predict a deflection within a precision in a range of 1 mm.

Table 7 Dependency of fitting precision on number of unit

Number of unit	5	10	15
Fitting precision*	under 0.07	under 0.04	0.05

* Normalized error

Table 8 Dependency of prediction ability on number of data set

Number of learning data		30	40	50
Maximum prediction error	X (mm)	3.46	1.72	1.66
	Y (mm)	2.30	1.51	0.97
	ϕ (deg.)	0.046	0.030	0.032

(2) Compensation ability

According to the neural network predictor defined from the above sensitivity study, a simulation on position compensation control of the manipulator tip is carried out. In this simulation, the target tip positions are fixed at the positions shown in Fig. 5 (b) and the target tip angle is specified to be 0 degree for all cases.

Table 9 shows the simulation results as a function of number of learning data set. It is found from Table 9 that a deflection between the target position and the actual trip position of the manipulator can be significantly decreased by using the neural network predictor and the prediction precision is increased with increase in the number of learning data set: in case of the learning data set of 40, the deflection of the tip position and angle against the target values can be compensated within an accuracy of 1 mm and 10^{-2} degree, respectively.

Table 9 Simulation results of position/posture compensation

Target position	Rigid model simulation without compensation	Neural network simulation		
		Number of learning data set (30)	Number of learning data set (40)	Number of learning data set (50)
1	9.93 2.00	0.846 -0.117	0.373 5.48×10^{-4}	0.338 -2.52×10^{-2}
2	18.2 2.51	3.87 -0.135	0.940 -2.45×10^{-3}	1.13 -4.64×10^{-3}
3	15.5 2.40	3.68 -0.118	0.756 $9.92\times^{-}10^{4}$	0.770 2.34×10^{-2}
4	15.3 2.41	3.52 -0.104	0.547 -3.61×10^{-4}	0.553 -1.71×10^{-2}
5	20.0 2.61	3.47 -0.151	0.690 -1.66×10^{-2}	0.176 -2.37×10^{-2}

Upper value: position precision (mm), Lower value: angle precision (deg.)

5. BENCHMARK EXPERIMENTS

In order to validate the simulation results, benchmark experiments using the sub-scaled manipulator are conducted with the same conditions as those of the simulation. In the benchmark experiments, two region, A and B, are selected as the working space of the manipulator tip as shown in **Fig. 6**. In the region A, the manipulator arms have to be extended with horizontal posture, so that a higher deflection of the tip is expected more than the case of the region B.

Table 10 shows the benchmark experiment results obtained in each working space, together with target positions and angles of the manipulator tip. In Table 10, the rigid model control indicates the results without compensation by the neural network predictor and the manipulator is just moved along the joint angles obtained from inverse kinematics of the rigid model. In case of the neural network control, those tip positions and angles obtained from the rigid model are compensated with the neural network predictor. As a result, it has been demonstrated that the neural network predictor gives significant improvement on the position/posture control of a flexible manipulator, as expected in the simulation. By comparing the neural network control with the rigid model control, the control precision of the tip position and angle is increased in order of a figure.

Table 9 Simulation results of position/posture compensation

Target position	Rigid model simulation without compensation	Neural network simulation		
		Number of learning data set (30)	Number of learning data set (40)	Number of learning data set (50)
1	9.93 2.00	0.846 -0.117	0.373 5.48×10^{-4}	0.338 -2.52×10^{-2}
2	18.2 2.51	3.87 -0.135	0.940 -2.45×10^{-3}	1.13 -4.64×10^{-3}
3	15.5 2.40	3.68 -0.118	0.756 $9.92\times^{-}10^{4}$	0.770 2.34×10^{-2}
4	15.3 2.41	3.52 -0.104	0.547 -3.61×10^{-4}	0.553 -1.71×10^{-2}
5	20.0 2.61	3.47 -0.151	0.690 -1.66×10^{-2}	0.176 -2.37×10^{-2}

Upper value: position precision (mm), Lower value: angle precision (deg.)

5. BENCHMARK EXPERIMENTS

In order to validate the simulation results, benchmark experiments using the sub-scaled manipulator are conducted with the same conditions as those of the simulation. In the benchmark experiments, two region, A and B, are selected as the working space of the manipulator tip as shown in **Fig. 6**. In the region A, the manipulator arms have to be extended with horizontal posture, so that a higher deflection of the tip is expected more than the case of the region B.

Table 10 shows the benchmark experiment results obtained in each working space, together with target positions and angles of the manipulator tip. In Table 10, the rigid model control indicates the results without compensation by the neural network predictor and the manipulator is just moved along the joint angles obtained from inverse kinematics of the rigid model. In case of the neural network control, those tip positions and angles obtained from the rigid model are compensated with the neural network predictor. As a result, it has been demonstrated that the neural network predictor gives significant improvement on the position/posture control of a flexible manipulator, as expected in the simulation. By comparing the neural network control with the rigid model control, the control precision of the tip position and angle is increased in order of a figure.

Table 10 Benchmark experiment results on position control

Working space	Target position/angle				Rigid model control			Neural network control		
	No.	X *mm*	Y *mm*	θ deg.	X *mm*	Y *mm*	θ deg.	X *mm*	Y *mm*	θ deg.
A	1	1450	-150	-45	1444.1	-161.6	-46.2	1450.4	-150.8	-44.9
	2	1550	0	-22	1545.8	-15.5	-24.0	1550.4	-1.1	-22.0
	3	1550	150	-6	1448.5	133.9	-9.8	1551.3	148.3	-6.3
B	4	1000	-500	-100	1002.1	-505.1	-99.0	1000.0	-500.5	-99.9
	5	1150	-350	-70	1147.3	-355.0	-70.3	1149.5	-350.5	-70.0
	6	1300	-200	-61	1295.8	-207.1	-61.7	1299.8	-200.5	-61.1

6. CONCLUSIONS

A sub-scaled model of flexible manipulator has been fabricated in order to develop an autonomous position-posture control method required for the in-vessel maintenance such as viewing, inspection and limiter handling in fusion experimental reactors. The design parameters of the manipulator are chosen from the current ITER design concept and the mechanical characteristics such as deflection and natural frequency have been measured.

A new position control method using a combination of neural network predictor with a rigid inverse kinematics has been proposed so as to simplify a kinematics modeling, to enable quick position compensation in stead of ordinary large matrix compensation, and to be applicable to a wide variety of manipulator characteristics. Through analytical simulation and benchmark experiments using the flexible manipulator, it has been concluded that the new position control method gives significant improvement in control performance with high precision in order of a figure. In addition, further optimization can be possible by adding other non-linear predictors such as radial basis function and fuzzy modeling.

As a whole, the basic feasibility of the neural network control has been quantitatively demonstrated and the control precision for compensating a deflection of a flexible manipulator has been qualified. Further optimization and qualification are being planned including a mock-up test of a 1/1-scaled manipulator.

Table 10 Benchmark experiment results on position control

Working space	Target position/angle				Rigid model control			Neural network control		
	No.	X *mm*	Y *mm*	θ deg.	X *mm*	Y *mm*	θ deg.	X *mm*	Y *mm*	θ deg.
A	1	1450	-150	-45	1444.1	-161.6	-46.2	1450.4	-150.8	-44.9
	2	1550	0	-22	1545.8	-15.5	-24.0	1550.4	-1.1	-22.0
	3	1550	150	-6	1448.5	133.9	-9.8	1551.3	148.3	-6.3
B	4	1000	-500	-100	1002.1	-505.1	-99.0	1000.0	-500.5	-99.9
	5	1150	-350	-70	1147.3	-355.0	-70.3	1149.5	-350.5	-70.0
	6	1300	-200	-61	1295.8	-207.1	-61.7	1299.8	-200.5	-61.1

6. CONCLUSIONS

A sub-scaled model of flexible manipulator has been fabricated in order to develop an autonomous position-posture control method required for the in-vessel maintenance such as viewing, inspection and limiter handling in fusion experimental reactors. The design parameters of the manipulator are chosen from the current ITER design concept and the mechanical characteristics such as deflection and natural frequency have been measured.

A new position control method using a combination of neural network predictor with a rigid inverse kinematics has been proposed so as to simplify a kinematics modeling, to enable quick position compensation in stead of ordinary large matrix compensation, and to be applicable to a wide variety of manipulator characteristics. Through analytical simulation and benchmark experiments using the flexible manipulator, it has been concluded that the new position control method gives significant improvement in control performance with high precision in order of a figure. In addition, further optimization can be possible by adding other non-linear predictors such as radial basis function and fuzzy modeling.

As a whole, the basic feasibility of the neural network control has been quantitatively demonstrated and the control precision for compensating a deflection of a flexible manipulator has been qualified. Further optimization and qualification are being planned including a mock-up test of a 1/1-scaled manipulator.

ACKNOWLEDGMENTS

The authors would like to express their sincere appreciation to Drs. S. Shimamoto and S. Matsuda for their continuous encouragement on this work. The contributions by the staffs of department of ITER project and Toshiba Corp., are gratefully acknowledged.

REFERENCES

[1] S. Matsuda, et al: Proc. 13th Conf. on Plasma Physics and Controlled Nuclear Fusion Research, (Washington, 1990) IAEA-CN-53/G-2-2.

[2] K. Tomabechi: Proc. 13th Conf. on Plasma Physics and Controlled Fusion Research (Washington, 1990), IAEA-CN-53/F-1-1.

[3] T. A. Johnasen and B. A. Foss: Representing and learning unmodelled dynamics with neural network memories, in preprints of ACC, pp.3037-3043(1992).

FIGURE CAPTIONS

Fig. 1 Schematic view of in-vessel manipulator in ITER

Fig. 2 An overall assembly of sub-scaled model of flexible manipulator

Fig. 3 Structural view of sub-scaled flexible manipulator

Fig. 4 Control algorithm for position compensation using neural network

Fig. 5 Analytical simulation model and working space

Fig. 6 A setup of benchmark experiments

ACKNOWLEDGMENTS

The authors would like to express their sincere appreciation to Drs. S. Shimamoto and S. Matsuda for their continuous encouragement on this work. The contributions by the staffs of department of ITER project and Toshiba Corp., are gratefully acknowledged.

REFERENCES

[1] S. Matsuda, et al: Proc. 13th Conf. on Plasma Physics and Controlled Nuclear Fusion Research, (Washington, 1990) IAEA-CN-53/G-2-2.

[2] K. Tomabechi: Proc. 13th Conf. on Plasma Physics and Controlled Fusion Research (Washington, 1990), IAEA-CN-53/F-1-1.

[3] T. A. Johnasen and B. A. Foss: Representing and learning unmodelled dynamics with neural network memories, in preprints of ACC, pp.3037-3043(1992).

FIGURE CAPTIONS

Fig. 1 Schematic view of in-vessel manipulator in ITER

Fig. 2 An overall assembly of sub-scaled model of flexible manipulator

Fig. 3 Structural view of sub-scaled flexible manipulator

Fig. 4 Control algorithm for position compensation using neural network

Fig. 5 Analytical simulation model and working space

Fig. 6 A setup of benchmark experiments

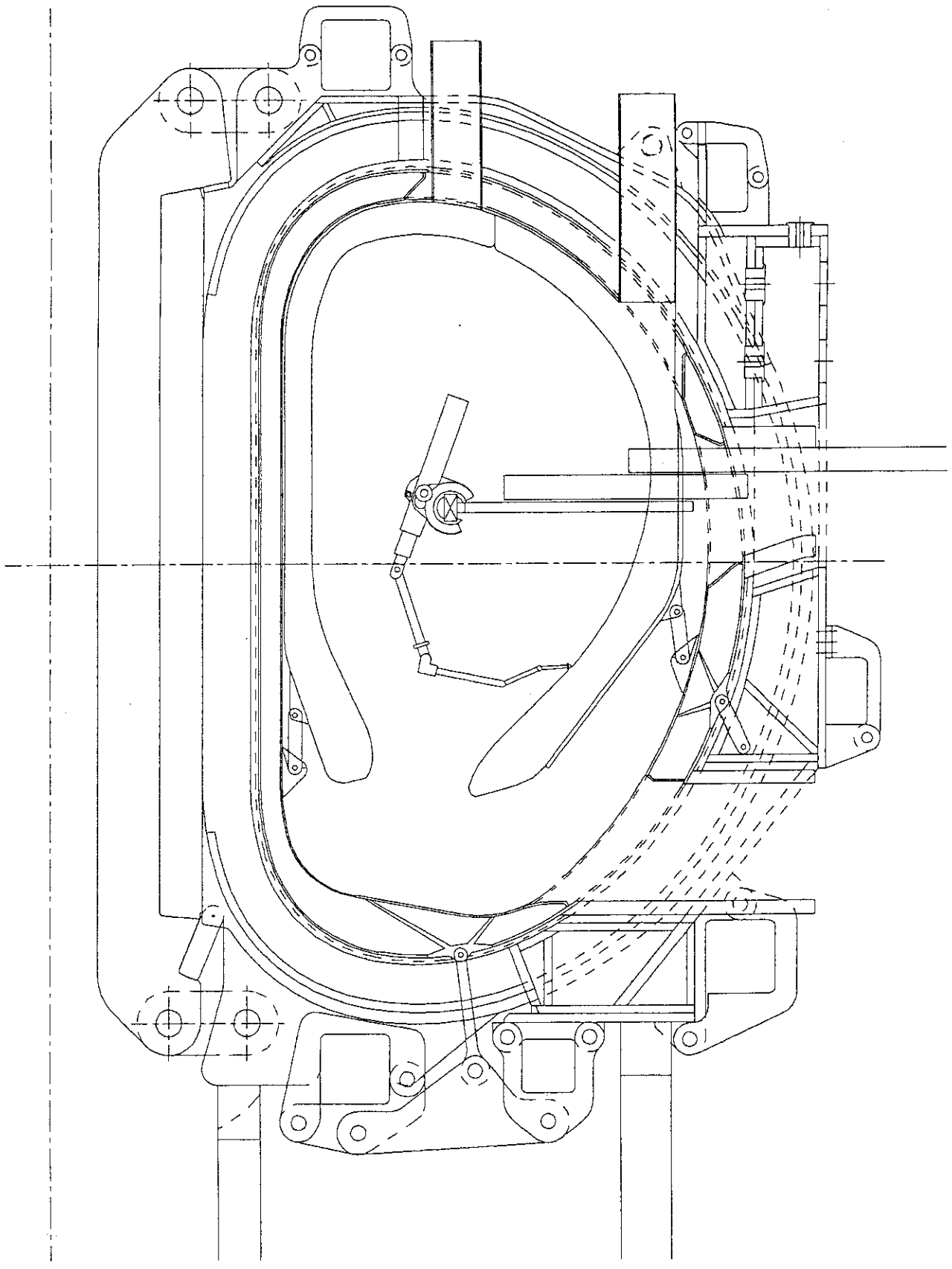

Fig. 1 Schematic view of in-vessel manipulator in ITER

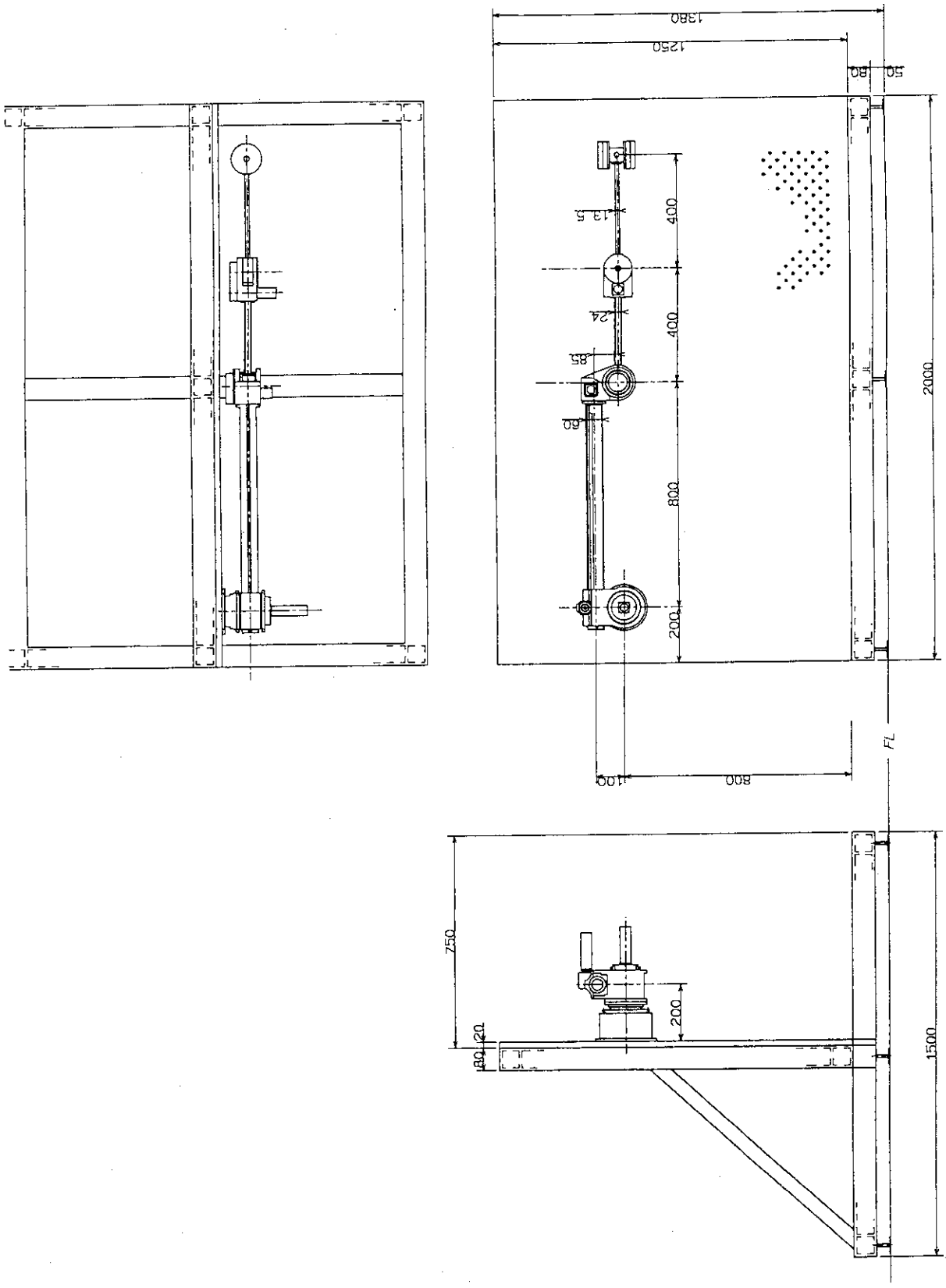

Fig. 2 An overall assembly of sub-scaled model of flexible manipulator

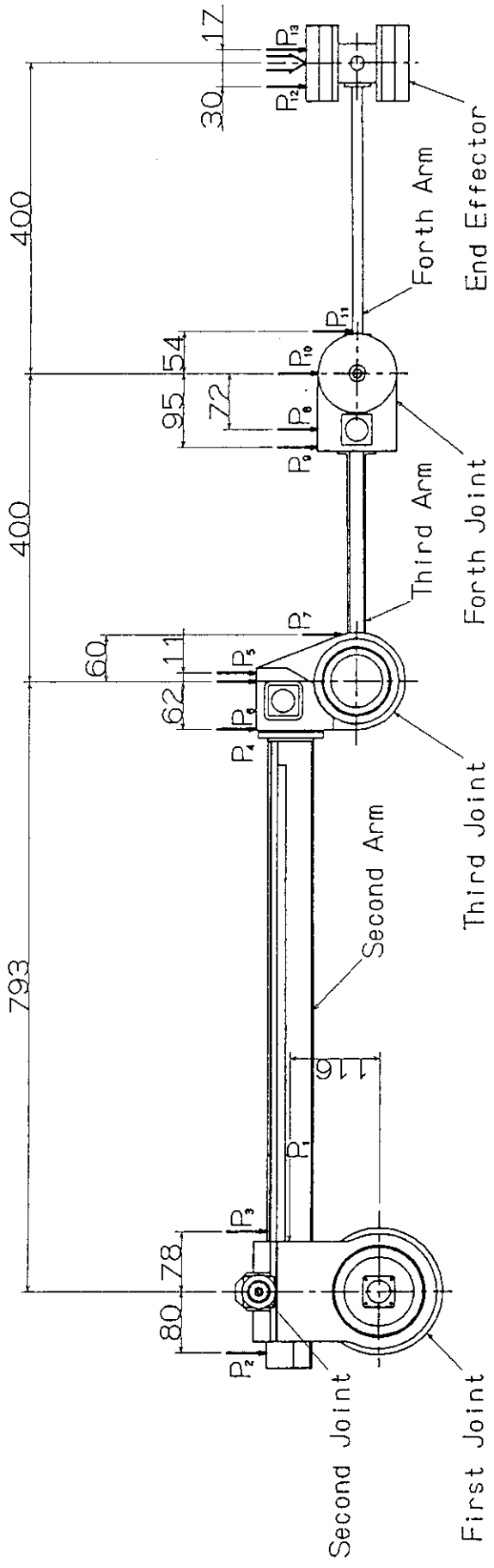

Fig. 3 Structural view of sub-scaled flexible manipulator

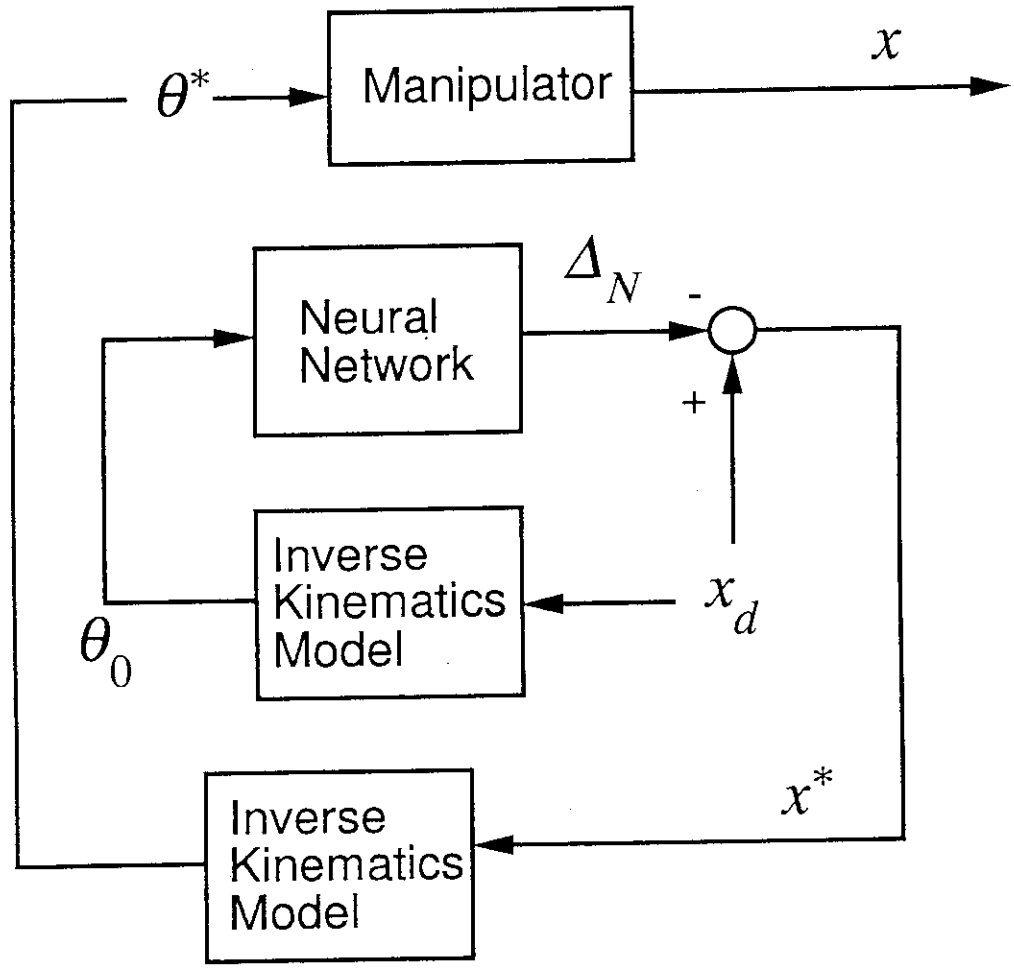

Fig. 4 Control algorithm for position compensation using neural network

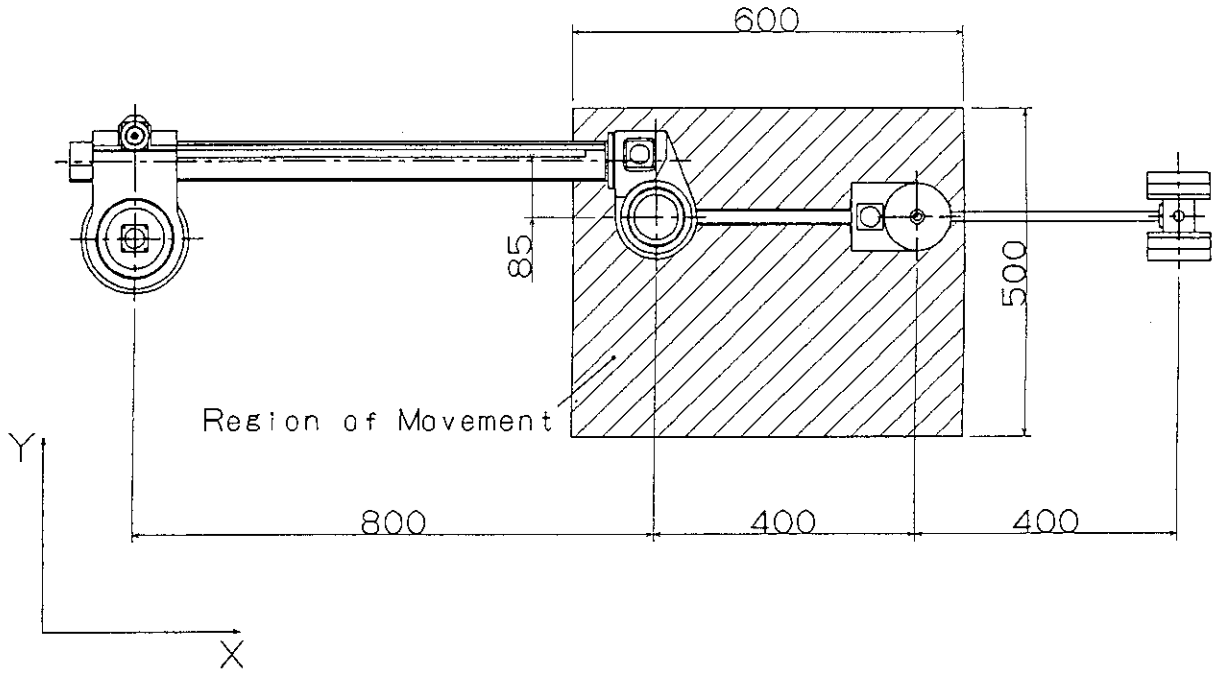

(a) Working space

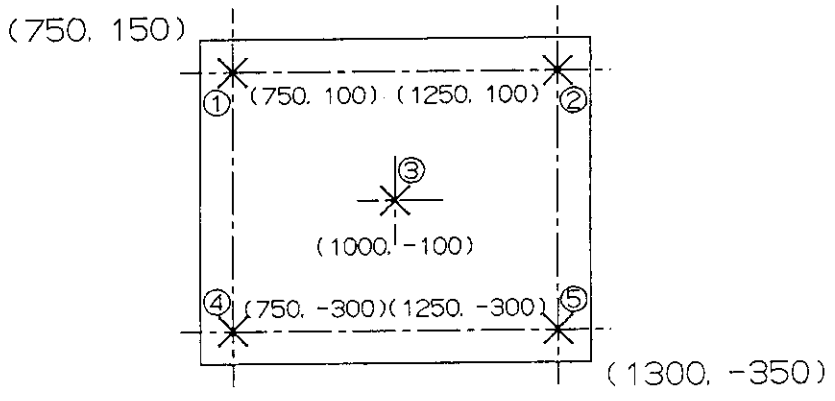

(b) Target position (①～⑤) in the working space

Fig. 5 Analytical simulation model and working space

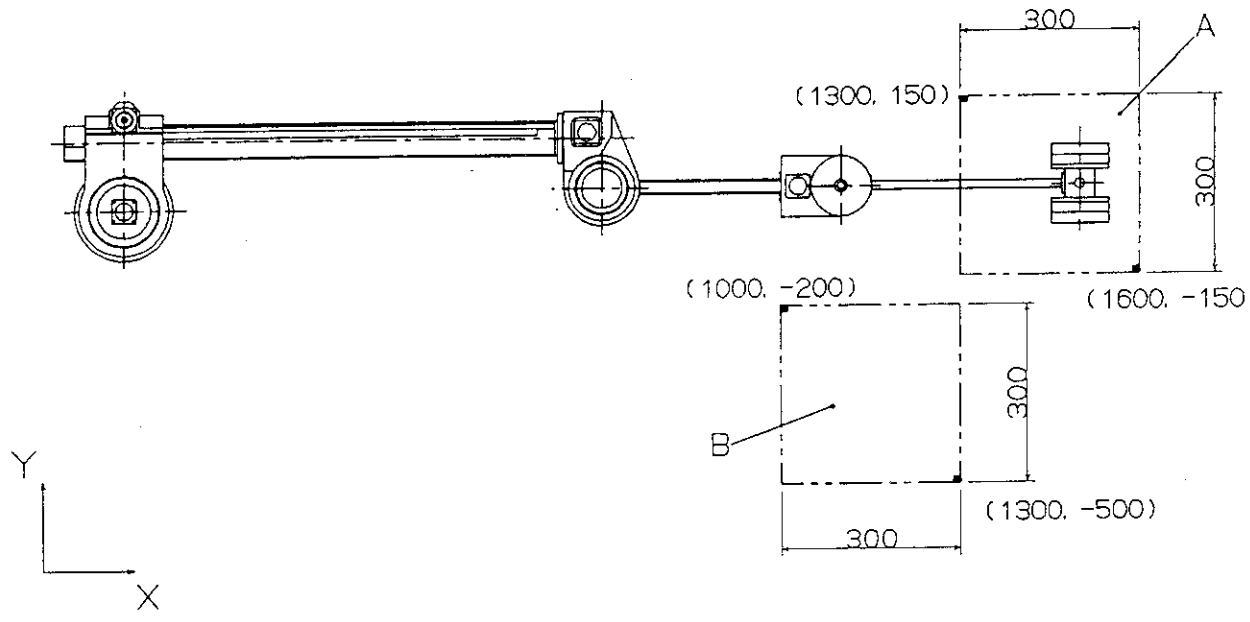

Fig. 6 A setup of benchmark experiments